*Journal of Ceramic Processing Research. Vol. 16, No. 2, pp. 249~257 (2015)*

J O U R N A L O F
**Ceramic Processing Research**

# Optimization of EDM parameters for $ZrO_2$ and $Al_2O_3$ ceramics using Taguchi method

**Yan-Cheng Lin[a,*], Jung-Chou Hung[b], Han-Ming Chow[c] and A-Cheng Wang[d]**

[a,c]*Department of Mechanical Engineering, Nan Kai University of Technology, Nantou 54243, Taiwan*
[b]*Department of Mechanical and Computer-Aided Engineering, Feng Chia University, Taichung 40724, Taiwan*
[d]*Department of Mechanical Engineering, Chien Hsin University of Science and Technology, Taoyuan 32097, Taiwan*

**Electrical Discharge Machining (EDM) is the most commonly used technique in mold and die manufacturing. The purpose of this investigation was to optimize the machining parameters of EDM on zirconium dioxide ($ZrO_2$) and aluminum oxide ($Al_2O_3$). During the EDM process, the surface of electrically nonconductive ceramic was covered with adhesive conductive copper (Cu) and aluminum (Al) foils to attain the threshold of electrical conductivity for the EDM process. The machining characteristics associated with the EDM process such as material removal rate (MRR) and surface roughness (SR) were explored through the experimental study according to an L18 orthogonal array using the Taguchi method. The analysis of variance (ANOVA) was conducted to examine the significant machining parameters which affect the machining characteristics. As the experimental results show, peak current and pulse duration significantly affected MRR and SR. In addition, the optimal combination levels of machining parameters were also determined from the response graph of signal-to-noise (S/N) ratios for each level of machining parameters. A practical and convenient process for shaping the electrically nonconductive ceramics was developed which featured high efficiency, high precision, and high-quality of surface integrity.**

**Key words: EDM, Taguchi method, Material removal rate, Surface roughness, Nonconductive ceramics, ANOVA.**

## Introduction

A non-conventional machining process, electrical discharge machining (EDM), has been frequently applied on developing precise and finished parts in industries. The EDM process removes surplus materials by means of consecutive sparks (discharge columns) produced between tool electrode and workpiece, which are separated by a dielectric fluid such as kerosene and deionized water. During the EDM process, an extremely elevated temperature is generated by the consecutive electrical sparks when the electrical power is supplied to tool electrode and workpiece, if the gap condition is suitable for developing the discharge column. The partial amount of workpiece material and tool electrode on a sparking spot is vaporized and melted due to the high temperature. Then, an impulsive force is developed by the dielectric fluid explosion, and the melted materials are ejected from the machined surface due to the local impulsive force. It is well known that the material removal effects caused by vaporizing, melting, and dielectric explosion are not governed by the mechanical properties of the workpiece such as strength, toughness, and hardness. Consequently, the EDM process is adequate to be employed in machining difficult-to-machine materials such as mold steels, high speed steels, cemented carbides, and ceramics [1-4].

Ceramics have diverse applications in many industrial fields such as molds and dies, machining tools, electronic devices, and semiconductor systems. The versatile features and sophisticated characteristics of ceramics are attributed to its excellent physical and mechanical properties. Although ceramics with outstanding properties such as high strength, distinguished hardness, excellent dielectric strength, and superior corrosion resistance could promote their service performance in various fields, it also reveals tough challenges in the traditional machining stage due to the increased cost.

Several researchers have conducted EDM experiments on ceramics machining and the results confirmed that thermal spalling is one of the main material removal mechanisms for machining conductive ceramics [5-7]. Hocheng *et al*. [8] reported that the material removal rate (MRR) was higher when the EDM machining parameters were set at a larger peak current and shorter pulse duration for machining SiC/Al composite material. Pitman *et al*. [9] and Liu *et al*. [10] indicated that surface defects like micro-cracks and pocked craters would show on the machined surface after EDM process performed on ceramic materials, and the surface defects would inevitably degraded the service performance and usage endurance of a component. Puertas *et al*. [11] and Luis *et al*. [12] also suggested the statistical analysis methods to analyze the optimization of the EDM

*Corresponding author:
Tel : +886-49-2563489
Fax: +886-49-2563788
E-mail: ycline@nkut.edu.tw

parameters to improve the machining characteristics for ceramic materials. Although the EDM process exhibits a noticeable performance for machining the difficult-to-machine materials such as ceramics and composites, the main EDM applications in ceramic machining are confined to electrically conductive ceramics. However, the major electrically non-conductive ceramics that are most frequently used in modern industrial fields such as zirconium dioxide ($ZrO_2$) and aluminum oxide ($Al_2O_3$) also revealed the rigorous limitations associated with choosing a suitable machining process with reasonable efficiency and quality. Mohri and coworkers [13-15] proposed a novel approach called the assistant electrode method using metal mesh, metal plate, PVD coating layer, and baked colloidal graphite on the workpiece surface to overcome the threshold of electrical conductivity for EDM process. In this approach, the initial electrical discharges could be constructed in the machining gap between the tool electrode and the assistant conductive materials covered on the ceramic workpiece, and then the pyrolytic carbon cracked from kerosene would deposit on the machined surface of the electrically non-conductive ceramics to reach the threshold of electrical conductivity for EDM progress. The experimental results show that the baked colloidal graphite and PVD coating layer methods would produce outstanding machining performance for electrically non-conductive ceramics. However, the baked and PVD processes inevitably needs some additional facilities and intensive operating time, and the operation costs would unavoidably increase for machining electrically non-conductive ceramics. For each practical approach introduced and employed in the EDM process, the efforts are focused on obtaining better product quality, improving the capability of machining characteristics, exploiting new technique to extend the applications of EDM process. The technical challenge in EDM for processing electrically non-conductive ceramics is to develop a robust and efficient electrically conductive layer created on the machined surface to maintain the EDM progress.

In this investigation, the essential EDM parameters such as type of adhesive foil (Type), peak current ($I_p$), auxiliary current with high voltage ($I_H$), pulse duration ($\tau_p$), electrode jumping interval (EJI), and servo reference voltage ($S_v$) were varied according to an $L_{18}$ orthogonal array based on the Taguchi experimental design to determine their effects on MRR and SR. In addition, the experimental data were transferred to signal-to-noise (S/N) ratios and machining parameters were evaluated by the analysis of variance (ANOVA) and the optimal combination levels of machining parameters for MRR and SR were obtained. Therefore, a sophisticated process with high efficiency, high accuracy and high quality of surface integrity was achieved to evolve the EDM applications for shaping electrically non-conductive ceramics with practical features to fit the modern industrial requirements.

## Experimental Method

### Taguchi parameter design

A systematic and statistical approach was effective and efficient to optimize machining parameters of the EDM process. Therefore, a design of experiment (DOE) was adopted to optimize the EDM parameter settings for $ZrO_2$ and $Al_2O_3$ ceramics using the Taguchi parameter design in this study. The procedures of the Taguchi parameter design are presented as follows:

1. Selection of the quality characteristics

There are three types of quality characteristics in the Taguchi method, such as smaller-the-better (STB), larger-the-better (LTB), and nominal-the-best (NTB). In this study, the goals were to maximize quality characteristics such as MRR and to minimize SR, therefore, both of the smaller-the-better and larger-the-better quality characteristics were introduced and implemented.

2. Selection of noise factors and control factors

The control factors including type of adhesive foil (Type), peak current ($I_p$), auxiliary current with high voltage ($I_H$), pulse duration ($\tau_p$), electrode jumping interval (EJI), and servo reference voltage ($S_v$) were considered as possible factors impacting the quality characteristics.

3. Selection of orthogonal array

There are 18 basic types of standard orthogonal arrays (OA) in the Taguchi method. Since six factors were studied in this investigation, five factors with three levels and one factor with two levels were considered. Therefore, an L18 orthogonal array was selected for this study.

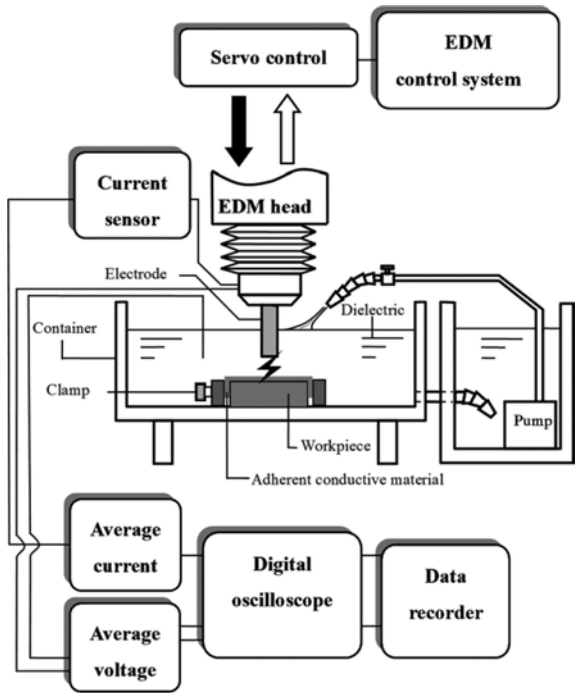


**Fig. 1.** Schematic diagram of experimental setup.

4. Conducting the experiments

There are 18 runs of experiments conducted in a CNC controlled die sinking EDM machine (model CM 323C made by CHMER Corp. in Taiwan) during this investigation. The stability of EDM progress was determined by inspecting discharge waveforms. Thus, a fast digital oscilloscope (Tektronix TD 2014) was employed in the experiments, which was coupled with a current probe (Chauvin Arnoux E3N) and a passive voltage probe (P2200) to detect the waveforms of discharge current and voltage during the EDM process. The schematic diagram of the experimental setup is shown in Fig. 1.

5. Analyzing the results and determining the optimum machining parameters

After raw data were collected, S/N response ratios was calculated. The L18 orthogonal array had eight columns and 18 rows, so it had 17 degrees of freedom to manipulate one parameter with two levels and seven parameters with three levels. In this study, two observed values of MRR and SR were explored. The levels of each machining parameter were set in accordance with the L18 orthogonal array. The experimentally observed MRR values are the larger-the-better (LTB) quality characteristics and SR values are the smaller-the-better (STB) quality characteristics. Therefore, the optimal observed MRR was its maximum value, and the optimal SR values, in contrast, were the minimum value.

Based on the Taguchi parameter design, the S/N ratio calculation was chosen as the larger-the-better (LTB) and the smaller-the-better (STB) as given in the following equations [16, 17]:

$$\text{LTB: } \eta = -10\log\left[\frac{1}{n}\sum_{i=1}^{n} yi^{-2}\right] \quad \text{(Eq.1)}$$

$$\text{STB: } \eta = -10\log\left[\frac{1}{n}\sum_{i=1}^{n} yi^{2}\right] \quad \text{(Eq.2)}$$

Where $\eta$ denotes the S/N ratio calculated from the observed values (unit: dB), $y_i$ represents the experimentally observed value of the *i* th experiment, and n is the repeated number of each experiment. Notably, each experiment in the L18 array is conducted three times in this investigation. Then, the optimum level combination based on the S/N ratios was calculated after the response table was created.

## Experimental materials

High purity of $ZrO_2$ and $Al_2O_3$ ceramics were adopted as workpiece materials in this investigation, which are widely used in modern industrial applications due to their excellent corrosion resistance, good hardness, and exceptional strength at high temperatures. The electrode material employed electrolytic copper for this work. The dimensions of workpiece and electrode were 12 mm × 12 mm × 5 mm and 30 mm × 20 mm × 1.5 mm, respectively. Thus, a machined area of 1.5 mm × 5 mm would be formed on the machined surface of workpiece. The essential properties of $ZrO_2$ and $Al_2O_3$ ceramics as well as copper electrode are listed in Tables 1 and 2.

**Table 1.** Essential properties of copper electrode.

| Properties | Descriptions |
|---|---|
| Specific gravity (g/cm$^3$) | 8.94 |
| Melting range (°C) | 1065-1083 |
| Thermal conductivity (W/m K) | 388 |
| Specific heat capacity (J/g °C ) | 0.385 |
| Thermal expansion coefficient (1/°C) | $1.7 \times 10^{-5}$ |
| Electrical resistivity (Ω cm) | $1.7 \times 10^{-6}$ |

**Table 2.** Essential properties of $ZrO_2$ and $Al_2O_3$.

| Workpiece materials | $Al_2O_3$ | $ZrO_2$ |
|---|---|---|
| Specific gravity (g/cm$^3$) | 3.96 | 5.68 |
| Thermal conductivity (W/m K) | 30-40 | 2 |
| Electrical resistivity (Ω cm) | $> 10^{14}$ | $10^{10}$ |
| Melting point (°C) | 2050 | 2720 |
| Specific heat capacity (J/g °C ) | 0.75-0.85 | 0.4 |
| Thermal expansion coefficient (1/°C) | $5.5 \times 10^{-6}$ | $7.0 \times 10^{-6}$ |
| Hardness (Hv) | 1760 | 1270 |

**Table 3.** Essential properties of adhesive Cu and Al foils.

| Properties | Cu | Al |
|---|---|---|
| Foil thickness (mm) | 0.035 | 0.05 |
| Adhesive thickness (mm) | 0.025 | 0.03 |
| Total thickness (mm) | 0.06 | 0.08 |
| Adhesion to steel (N/cm) | 4.5 | 4.0 |
| Tensile strength (N/cm) | 40 | 18 |
| Temperature resistance (°C) | −20 to 155 up | −20 to 155 up |
| Electrical resistance through adhesive (Ω cm) | 0.003 | 0.02 |

The end face of electrode against the workpiece was ground on a plate using emery paper in a sequence of mesh 600#, 800#, and 1200# to guarantee the surface finishing and the flatness of each electrode at the same condition. The experiments were performed in a kerosene dielectric (commercial grade) covered specimens with 20 mm. Since the workpiece materials $ZrO_2$ and $Al_2O_3$ were electrically non-conductive ceramics, the machined surface of $ZrO_2$ and $Al_2O_3$ ceramics should be covered by an assisted electrically conductive material to reach the threshold of electrical conductivity for EDM process and to form the electrical discharge columns between the tool electrode and workpiece at the initial stage of EDM process. Consequently, the pyrolytic carbon cracked from kerosene was produced and deposited on the machined surface of $ZrO_2$ and $Al_2O_3$ ceramics. Moreover, the tool electrode composition would be transferred to machine surface during EDM process

[18, 19], and then the migrated tool electrode composition could improve the required conductive layer to be constructed on the workpiece surface. For the purpose of reducing the operational complexity, the assisted electrically conductive material in this work employed adhesive copper and aluminum foils whose specifications and properties are listed in Table 3. The adhesive copper and aluminum foils could be firmly adhered on the electrically non-conductive ceramics without any additional operations, and the crucial constraint associated with the electrical conductivity for EDM process was constructed on electrically non-conductive ceramic materials.

**Table 4.** Experimental conditions in EDM.

| Working conditions | Descriptions |
|---|---|
| Workpiece | $ZrO_2$(+) , $Al_2O_3$ (+) |
| Electrode | Cu (–) |
| Adhesive foil | Cu, Al |
| Peak current, ($I_P$) | 2, 3, 4 A |
| Pulse duration, ($\tau_P$) | 50, 100, 200 μs |
| Auxiliary current with high voltage, ($I_H$) | 0.4, 0.9, 1.2 A |
| No load voltage, ($V_o$) | 140 V |
| Servo reference voltage, ($S_V$) | 40, 55, 70 V |
| Electrode jumping interval, (EJI) | 2, 3, 4 sec |
| Electrode jumping height | 2 mm |
| Duty factor, (D.F) | 0.5 |
| Dielectric fluid | Kerosene (Commercial grade) |
| Working time, (WT) | 30 min |

## Experimental equipment, measurements, and analysis

The machining characteristics such as MRR ($mm^3$/min) and SR (Ra, μm) were adopted to explore the effects of machining parameters on EDM characteristics of $ZrO_2$ and $Al_2O_3$ ceramics. The workpiece and electrode specimens were submerged in acetone and cleared by an ultrasonic cleaner for 5 minutes before and after each experiment, and then the specimens were weighed by an electronic balance (Precisa XT 220A) with 0.1 mg resolution to calculate the MRR. SR values

**Table 5.** Experimental observed values and levels of machining parameters in L18 orthogonal array.

| Observed values | Control parameters | Levels | | |
|---|---|---|---|---|
| • Material removal rate, MRR ($mm^3$/min)<br>• Surface roughness, SR (μm) | A. Adhesive foil (Type) | Cu | | Al |
| | B. Peak current ($I_p$) | 2 A | 30 A | 4 A |
| | C. Auxiliary current with high voltage ($I_H$) | 0.4 A | 0.98 A | 1.2 A |
| | D. Pulse duration ($\tau_p$) | 50 μs | 100 μs | 200 μs |
| | E. Electrode jumping interval, (EJI) | 2 sec | 3 sec | 4 sec |
| | F. Servo reference voltage ($S_v$) | 40 V | 55 V | 70 V |

**Table 6.** L18 orthogonal array, control parameters and S/N ratios.

| | Control factors | | | | | | | | S/N Ratios (η) | | | |
|---|---|---|---|---|---|---|---|---|---|---|---|---|
| | Type | $I_p$ | $I_H$ | $\tau_p$ | EJI | $S_v$ | $E_1$ | $E_2$ | $ZrO_2$ | | $Al_2O_3$ | |
| No. | (A) | (B) | (C) | (D) | (E) | (F) | (G) | (H) | MRR | SR | MRR | SR |
| 1 | Cu | 2 | 0.4 | 50 | 2 | 40 | 1 | 1 | –26.9856 | –14.2193 | –38.3169 | –21.2892 |
| 2 | Cu | 2 | 0.9 | 100 | 3 | 55 | 2 | 2 | –24.2195 | –16.6757 | –38.3169 | –23.7504 |
| 3 | Cu | 2 | 1.2 | 200 | 4 | 70 | 3 | 3 | –21.0194 | –20.8279 | –26.6164 | –23.8625 |
| 4 | Cu | 3 | 0.4 | 50 | 3 | 55 | 3 | 3 | –21.4105 | –16.4695 | –32.6370 | –23.1672 |
| 5 | Cu | 3 | 0.9 | 100 | 4 | 70 | 1 | 1 | –19.3813 | –18.4233 | –25.1787 | –23.7504 |
| 6 | Cu | 3 | 1.2 | 200 | 2 | 40 | 2 | 2 | –15.9505 | –20.3407 | –22.6432 | –24.4335 |
| 7 | Cu | 4 | 0.4 | 100 | 2 | 70 | 2 | 3 | –16.8487 | –20.6524 | –23.6938 | –24.2438 |
| 8 | Cu | 4 | 0.9 | 200 | 3 | 40 | 3 | 1 | –12.1783 | –22.2387 | –19.9273 | –24.609 |
| 9 | Cu | 4 | 1.2 | 50 | 4 | 55 | 1 | 2 | –15.0811 | –17.3376 | –22.866 | –23.1793 |
| 10 | Al | 2 | 0.4 | 200 | 4 | 55 | 2 | 1 | –16.2607 | –17.9525 | –20.8604 | –23.3463 |
| 11 | Al | 2 | 0.9 | 50 | 2 | 70 | 3 | 2 | –45.0474 | –11.8657 | –46.6164 | –20.9844 |
| 12 | Al | 2 | 1.2 | 100 | 3 | 40 | 1 | 3 | –25.1346 | –13.6609 | –30.2255 | –21.2892 |
| 13 | Al | 3 | 0.4 | 100 | 4 | 40 | 3 | 2 | –24.1409 | –19.5178 | –35.0207 | –24.6903 |
| 14 | Al | 3 | 0.9 | 200 | 2 | 55 | 1 | 3 | –15.7397 | –20.7803 | –17.3684 | –24.1796 |
| 15 | Al | 3 | 1.2 | 50 | 3 | 70 | 2 | 1 | –43.4637 | –17.7072 | –31.0534 | –22.0074 |
| 16 | Al | 4 | 0.4 | 200 | 3 | 70 | 1 | 2 | –14.0919 | –21.9382 | –24.4722 | –27.9379 |
| 17 | Al | 4 | 0.9 | 50 | 4 | 40 | 2 | 3 | –16.3241 | –17.8196 | –32.9916 | –22.6452 |
| 18 | Al | 4 | 1.2 | 100 | 2 | 55 | 3 | 1 | –19.1140 | –21.2892 | –15.8349 | –26.0984 |

were measured using a precision profilometer (Mitutoyo Surfest 4) to determine the surface quality of the machined surface after EDM process. The value of SR was obtained by averaging the five measurements that were stochastically performed on the different positions of the machined surface. The surface integrity was also explored by a scanning electron microscope (SEM) to evaluate the influences of EDM discharge energy. The details of machining conditions conducted in this investigation are given in Table 4. The electrical conductivity of $ZrO_2$ and $Al_2O_3$ ceramics should be first manipulated to fit the requirements of the EDM process, the pyrolytic carbon cracked from kerosene could be regarded as a solution to construct a suitable electrically conductive layer on the machined surface of $ZrO_2$ and $Al_2O_3$ ceramics. The pyrolytic carbon was enhanced to deposit on the anode side during EDM process [20]. Therefore, in this work, the workpieces of $ZrO_2$ and $Al_2O_3$ ceramic were connected to anodic polarity to improve the workpiece surface attaining the threshold of electrical conductivity.

The statistical method was employed to analyze the experimental data by performing the analysis of variance (ANOVA) in order to identify significant factors. Table 5 presents the experimentally observed values, machining parameters (control parameters) and the levels of the machining parameters based on the Taguchi parameter design. The S/N ratios were calculated from the experimental observed values, according to Eqs. 1 and 2. The optimal combination levels of the machining parameters correlated with the EDM that yielded a higher MRR and a lower SR for processing $ZrO_2$ and $Al_2O_3$ ceramics were determined by analyzing the S/N ratios shown on Table 6.

## Results and Discussion

### Nonconductive materials machined by EDM process

The $ZrO_2$ and $Al_2O_3$ ceramics are nonconductive materials, so an appropriate electrically conductively layer should be formed on the $ZrO_2$ and $Al_2O_3$ to overcome the electrically conductivity threshold for EDM process. In this work, the adhesive copper and aluminum foils were covered on the workpiece surface to induce the consecutive electrical sparks in the machining gap at the initial stage of the EDM process. Consequently, the pyrolytic carbon cracked from kerosene and deposited on the machined surface would sustain the electrical sparks continually forming in the machining gap. Fig. 2 shows the discharge wave forms of $ZrO_2$ and $Al_2O_3$ ceramics obtained during machining elapsed time (20-25 minutes) under a smaller ($I_p$: 2A, $\tau_p$: 200 μs) and a larger ($I_p$: 6A, $\tau_p$: 200 μs) discharge energy levels. When the elapsed machining time was prolonged to a definite time value (about 3-5 minutes), the electrode exceeded the covered adhesive foils and penetrated into $ZrO_2$ and $Al_2O_3$ ceramics.

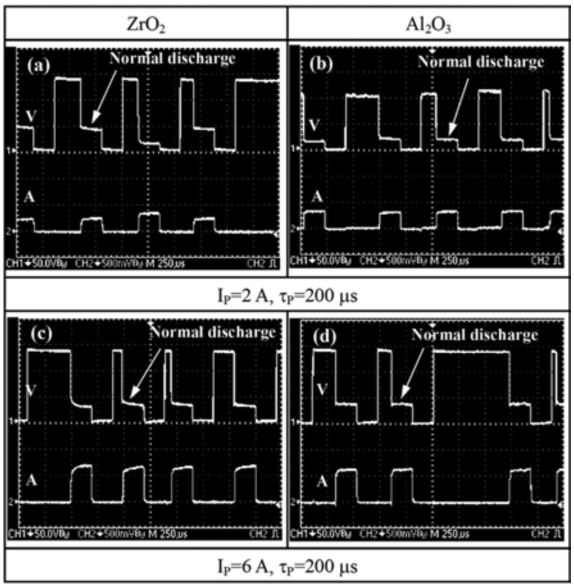


**Fig. 2.** Discharge waveforms of $ZrO_2$ and $Al_2O_3$ using adhesive copper foil (obtained during 20-25 min).

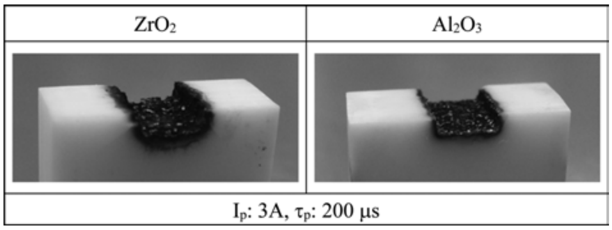


**Fig. 3.** Machined specimen of $ZrO_2$ and $Al_2O_3$ using EDM with adhesive copper foil. (Machining elapsed time 30 min).

As Fig. 2 shows, the discharge waveforms were not only obtained from $ZrO_2$ but also received from $Al_2O_3$ revealed normal discharge waveforms under smaller ($I_p$: 2A, $\tau_p$: 200 μs) and larger ($I_p$: 6A, $\tau_p$: 200 μs) discharge energy levels. The observations of discharge waveforms demonstrated that the electrically non-conductive ceramics which could be machined by EDM process covered an appropriate metal foil on the workpiece surface. Fig. 3 depicts the machined specimens of $ZrO_2$ and $Al_2O_3$ ceramics using EDM process covered a copper foil on the workpiece surface. The EDM process revealed the potential to shape the electrically non-conductive ceramics such as $ZrO_2$ and $Al_2O_3$. However, the relationships between the machining characteristics and the machining parameters should be comprehensively explored to meet the rigorous requirements for modern manufacturing applications.

### Optimizing machining parameter

Table 6 shows the S/N ratios of MRR and SR correlated with each experimental measurement of $ZrO_2$ and $Al_2O_3$ ceramics obtained from EDM process according to an $L_{18}$ orthogonal array based on the Taguchi method. Moreover, the S/N ratios were used to assess the effects of machining parameters (control

**Table 7.** ANOVA of MRR obtained from $ZrO_2$.

| Parameter (A) | Degree ($f_A$) | Square sum ($S_A$) | Variance ($V_A$) | $F_{A0}$ | $F_{0.05,n1,n2}$ |
|---|---|---|---|---|---|
| Type | 1 | 118.7966 | 118.7966 | 4.7866 | 5.99 |
| Ip | 2 | 373.9705 | 186.9853 | 7.5341* | 5.14 |
| $I_H$ | 2 | 34.5127 | 17.2564 | 0.6953 | 5.14 |
| $\tau_p$ | 2 | 445.9176 | 222.9588 | 8.9836* | 5.14 |
| EJI | 2 | 86.4495 | 43.2247 | 1.7416 | 5.14 |
| $S_v$ | 2 | 217.6329 | 108.8165 | 4.3845 | 5.14 |
| $E_{e1+e2}$ | 6 | 148.9105 | 24.8184 | | |

*Significant parameter.

**Table 8.** ANOVA of MRR obtained from $Al_2O_3$.

| Parameter (A) | Degree ($f_A$) | Square sum ($S_A$) | Variance ($V_A$) | $F_{A0}$ | $F_{0.05,n1,n2}$ |
|---|---|---|---|---|---|
| Type | 1 | 1.0021 | 1.0021 | 0.0349 | 5.99 |
| Ip | 2 | 316.4287 | 158.2144 | 5.5135* | 5.14 |
| $I_H$ | 2 | 92.4306 | 46.2153 | 1.6105 | 5.14 |
| $\tau_p$ | 2 | 439.1495 | 219.5748 | 7.6518* | 5.14 |
| EJI | 2 | 17.7937 | 8.8969 | 0.3100 | 5.14 |
| $S_v$ | 2 | 103.5103 | 51.7552 | 1.8036 | 5.14 |
| $E_{e1+e2}$ | 6 | 172.1727 | 28.6955 | | |

*Significant parameter.

parameters) on MRR and SR, by performing the analysis of variance (ANOVA). Thus, the significant parameters associated with each concerning machining characteristic would be determined. The optimal levels combination of the machining parameters to optimize MRR and SR were also determined from the S/N ratios response graphs.

*Material removal rate* (*MRR*)

Tables 7 and 8 displays the results of ANOVA of MRR based on S/N ratios obtained from $ZrO_2$ and $Al_2O_3$ ceramics respectively.

As the calculated results indicate that the significant machining parameters associated with MRR were peak current ($I_p$) and pulse duration ($\tau_p$) both from $ZrO_2$ and $Al_2O_3$ ceramics in EDM process. When the peak current and pulse duration were set at higher levels, the electrical discharge energies delivered into the machining zone were enlarged within a single pulse. The EDM process is a thermal erosion process, the main material removal mechanisms are melting, evaporation, and thermal spalling. The inherent properties of ceramics possess high hardness, high brittleness, as well as low thermal and electrical conductivity. Therefore, when ceramic materials were machined by EDM, the dramatic temperature gradient was easily generated during the process. Therefore, the removal mechanism of thermal spalling played a more dominant role in EDM process for ceramics than that for other materials. Consequently, when a larger amount of discharge energy delivered into the machining zone within single pulse, a higher

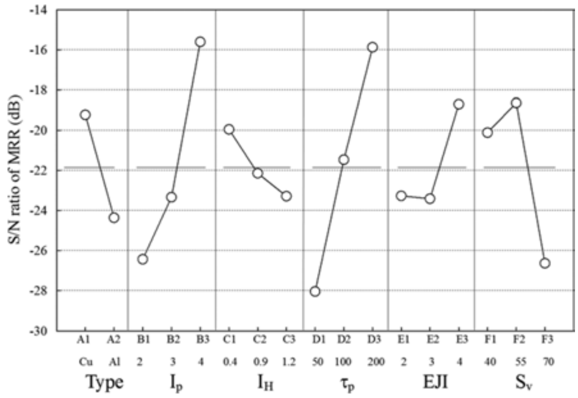


**Fig. 4.** S/N ratios response graph of MRR ($ZrO_2$).

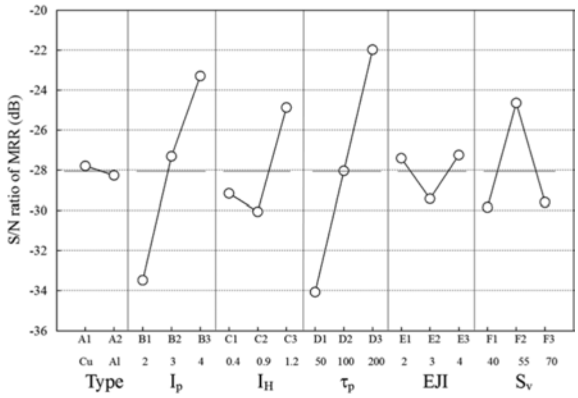


**Fig. 5.** S/N ratios response graph of MRR ($Al_2O_3$).

temperature would be produced in the machining zone. The effect of thermal spalling would be facilitated as a larger amount of discharge energy was supplied into the machining zone. It was well known that the discharge energy within single pulse was governed by peak current, machining voltage, and pulse duration. Therefore, if the peak current and pulse duration was set at higher levels, the large quantity of ceramic material would be removed from workpiece surface.

The MRR also revealed high values as the peak current and pulse duration set at high levels. In addition, the S/N ratios response graph of MRR plotted in Figs. 4 and 5 for indicating the optimal combination levels of the machining parameters of $ZrO_2$ and $Al_2O_3$ ceramics, individually. As Fig. 4 shows the optimal machining parameter levels for $ZrO_2$ ceramics in EDM process were: copper foil (Type); 4A peak current ($I_p$); 0.4A auxiliary current with high voltage ($I_H$); 200 μs pulse duration ($\tau_p$); 4 s electrode jumping interval (EJI); 55 V servo reference voltage ($S_v$). Fig. 5 demonstrates the S/N ratios response graph of MRR obtained from $Al_2O_3$ ceramics to indicate the optimal levels combination of machining parameters for maximum MRR. The optimal levels combination of machining parameters included copper foil (Type); 4 A peak current ($I_p$); 1.2 A auxiliary current with high voltage ($I_H$); 200 μs pulse duration ($\tau_p$); 4 s electrode jumping interval (EJI); 55 V servo reference voltage ($S_v$).

**Table 9.** ANOVA of SR obtained from $ZrO_2$.

| Parameter (A) | Degree ($f_A$) | Square sum ($S_A$) | Variance ($V_A$) | $F_{A0}$ | $F_{0.05,n1,n2}$ |
|---|---|---|---|---|---|
| Type | 1 | 1.2030 | 1.2030 | 0.4452 | 5.99 |
| Ip | 2 | 59.4304 | 29.7152 | 10.9960* | 5.14 |
| $I_H$ | 2 | 1.1190 | 0.5595 | 0.2070 | 5.14 |
| $\tau_p$ | 2 | 68.4717 | 34.2358 | 12.6680* | 5.14 |
| EJI | 2 | 0.9908 | 0.4954 | 0.1833 | 5.14 |
| $S_v$ | 2 | 1.1805 | 0.5902 | 0.2184 | 5.14 |
| $E_{e1+e2}$ | 6 | 16.2140 | 2.7023 | | |

*Significant parameter.

**Table 10.** ANOVA of SR obtained from $Al_2O_3$.

| Parameter (A) | Degree ($f_A$) | Square sum ($S_A$) | Variance ($V_A$) | $F_{A0}$ | $F_{0.05,n1,n2}$ |
|---|---|---|---|---|---|
| Type | 1 | 0.0444 | 0.0444 | 0.0300 | 5.99 |
| Ip | 2 | 16.8250 | 8.4125 | 5.6866* | 5.14 |
| $I_H$ | 2 | 2.1110 | 1.0555 | 0.7135 | 5.14 |
| $\tau_p$ | 2 | 19.9923 | 9.9961 | 6.7571* | 5.14 |
| EJI | 2 | 0.2258 | 0.1129 | 0.0763 | 5.14 |
| $S_v$ | 2 | 2.1249 | 1.0624 | 0.7182 | 5.14 |
| $E_{e1+e2}$ | 6 | 8.8761 | 1.4794 | | |

*Significant parameter.

*Surface roughness* (*SR*)

Tables 9 and 10 depict the results of ANOVA of SR based on S/N ratios associated with $ZrO_2$ and $Al_2O_3$ ceramics in EDM process, individually. As shown in the tables, the peak current ($I_p$) and pulse duration ($\tau_p$) were the significant parameters affecting SR both for $ZrO_2$ and $Al_2O_3$ ceramics in the EDM process. As mentioned above, when the peak current ($I_p$) and pulse duration ($\tau_p$) were set at high levels, a huge discharge energy would be delivered into the machining zone within a single pulse, so a large amount of workpiece material was removed due to the obvious material removal mechanisms that were generated in the machining zone.

As shown in Fig. 6, the SEM micrographs demonstrate that the machined surface presented coarser aspects (features) when the peak current ($I_p$) and pulse duration ($\tau_p$) were increased. Consequently, the SR became large when the peak current ($I_p$) and pulse duration ($\tau_p$) were set at a high levels. The S/N ratios response graphs of SR associated with $ZrO_2$ and $Al_2O_3$ ceramics were exhibited in Figs. 7 and 8 to reveal the optimal combination levels of machining parameters for minimum SR. Fig. 7 shows the optimal combination levels of machining parameters for $ZrO_2$ ceramics through EDM process including aluminum foil (Type); 2 A peak current ($I_p$); 0.9 A auxiliary current with high voltage ($I_H$); 50 μs pulse duration ($\tau_p$); 3 s electrode jumping interval (EJI); 40 V servo reference voltage ($S_v$). On the other hand, the optimal combination levels of machining parameters for $Al_2O_3$ ceramics through EDM process were depicted in

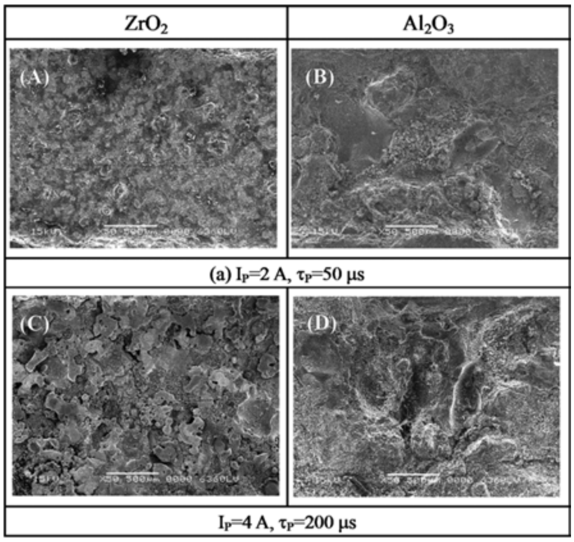


**Fig. 6.** SEM micrographs of $ZrO_2$ and $Al_2O_3$ machined surfaces.

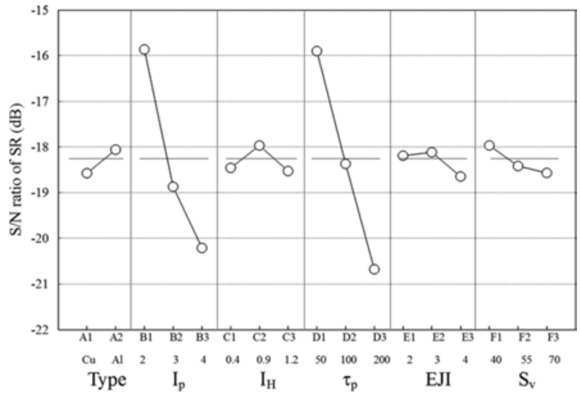


**Fig. 7.** S/N ratios response graph of SR ($ZrO_2$).

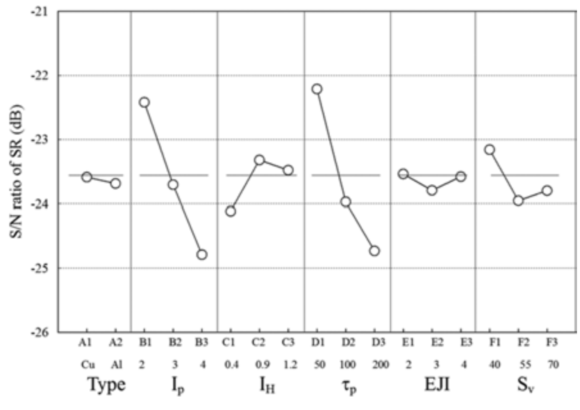


**Fig. 8.** S/N ratios response graph of SR ($Al_2O_3$).

Fig. 8. As shown in this plot, the optimal combination levels of machining parameters for minimum SR for $Al_2O_3$ ceramics through EDM process were as follows: copper foil (Type); 2 A peak current ($I_p$); 0.9 A auxiliary current with high voltage ($I_H$); 50 μs pulse duration ($\tau_p$); 2 s electrode jumping interval (EJI); 40 V servo reference voltage ($S_v$).

**Table 11.** Results of the confirmation experiments for $ZrO_2$.

| | | Initial levels of machining parameters | Optimal combination levels of machining parameters | |
|---|---|---|---|---|
| | | | Prediction | Experiment |
| MRR | level | $A_1B_2C_2D_2E_2F_2$ | $A_1B_3C_1D_3E_3F_2$ | $A_1B_3C_1D_3E_3F_2$ |
| | Observed values (mm$^3$/min) | 0.1074 | – | 0.2869 |
| | S/N ratio (dB) | –19.38 | –9.68 | –10.85 |
| SR | level | $A_1B_2C_2D_2E_2F_2$ | $A_2B_1C_2D_1E_2F_1$ | $A_2B_1C_2D_1E_2F_1$ |
| | Observed values (Ra/μm) | 8.34 | – | 3.37 |
| | S/N ratio (dB) | –18.42 | –13.45 | –10.55 |

**Table 12.** Results of the confirmation experiments for $Al_2O_3$.

| | | Initial levels of machining parameters | Optimal combination levels of machining parameters | |
|---|---|---|---|---|
| | | | Prediction | Experiment |
| MRR | level | $A_1B_2C_2D_2E_2F_2$ | $A_1B_3C_3D_3E_3F_2$ | $A_1B_3C_3D_3E_3F_2$. |
| | Observed values (mm$^3$/min) | 0.0551 | – | 0.1701 |
| | S/N ratio (dB) | –25.18 | –17.24 | –15.39 |
| SR | level | $A_1B_2C_2D_2E_2F_2$ | $A_1B_1C_2D_1E_1F_1$ | $A_1B_1C_2D_1E_1F_1$ |
| | Observed values (Ra/μm) | 15.40 | – | 7.70 |
| | S/N ratio (dB) | –23.75 | –20.10 | –17.73 |

**Confirmation experiment**

The optimal levels combination of the machining parameters were determined and confirmed as follows. The estimated S/N ratios are calculated as,

$$\hat{\eta} = \overline{\eta}_m + \sum_{i=1}^{n_o} (\overline{\eta}_i - \overline{\eta}_m) \quad (3)$$

$\hat{\eta}$ : Estimated S/N ratio for optimal levels combination of machining parameters.
$\overline{\eta}_m$ : Total mean of S/N ratio.
$n_0$ : The number of significant parameters.
$\overline{\eta}_i$ : Mean of S/N ratio at the optimal level.

Table 11 displays the results of confirmation experiments of $ZrO_2$ ceramics in EDM process with adhesive foils covered on the workpiece surface. As the results indicate that the S/N ratios correlated with MRR and SR for the optimal combination levels of machining parameters are 8.53 dB and 7.87 dB higher than those obtained at the initial experimental conditions $A_1B_2C_2D_2E_2F_2$. In addition, Table 12 reveals the results of confirmation experiments of $Al_2O_3$ ceramics using EDM process with adhesive foils covered on the workpiece surface. According to the results, the S/N ratios correlated with MRR and SR for the optimal combination levels of machining parameters are 9.79 dB, and 6.02 dB larger than those obtained at the initial experimental conditions $A_1B_2C_2D_2E_2F_2$. The experimental results confirm that the machining parameters of $ZrO_2$ and $Al_2O_3$ ceramics using EDM process with adhesive metal foils would be optimized for MRR and SR, so the observed values would thus be significantly improved.

## Conclusions

The effects of $ZrO_2$ and $Al_2O_3$ ceramics using EDM process with adhesive metal foils were determined and the optimal machining parameters of EDM process were estimated based on Taguchi method. According to the experimental results, and statistical analysis of ANOVA, the following conclusions have been drawn:

$ZrO_2$ and $Al_2O_3$ ceramics can be successfully machined in EDM process by covered electrically conductive aluminum and copper foils on the workpiece surfaces. The significant machining parameters associated with MRR were peak current ($I_p$) and pulse duration ($\tau_p$) both for $ZrO_2$ and $Al_2O_3$ ceramics using EDM process covered conductive foils on workpiece surfaces.

The peak current ($I_p$) and pulse duration ($\tau_p$) were the significant parameters affecting SR both for $ZrO_2$ and $Al_2O_3$ ceramics in EDM process with adhesively conductive foils.

In $ZrO_2$ ceramics using EDM process with adhesive metal foils, the S/N ratios correlated with MRR and SR for the optimal levels combination of machining parameters are 8.53 dB and 7.87 dB higher than those obtained at the initial experimental conditions.

The S/N ratios correlated with MRR and SR for the optimal levels combination of machining parameters to machine $Al_2O_3$ ceramics through EDM process are 9.79 dB and 6.02 dB larger than those obtained in the initial experimental conditions.

## Acknowledgments

The authors would like to thank the Ministry of

Science and Technology, Taiwan, Republic of China, for financially supporting this research under Contract No. NSC102-2221-E-252-002-MY3. The authors are also grateful to Mr. Li-Ran Shu at CCIT for his kindly assistance with experimental efforts.

## References

1. M. Kiyak, O. Cakir, J. Mater. Process. Technol. 191 (2007) 141-144.
2. B. Lauwers, J.P. Kruth, K. Brans, Ann. CIRP 56 [1] (2007) 225-228.
3. Y.C. Lin, Y.F. Chen, C.T. Lin, H.J. Tzeng, Mater. Manuf. Process. 23 (2008) 391-399.
4. Y.J. Lin, Y. Lin, A.C. Wang, D.A. Wang, H.M. Chow, Adv. Mater. Res. 154-155 (2011) 794-805.
5. Y.M. Cheng, P.T. Eubank, A.M. Gadalla, Mater. Manuf. Process. 11 [4] (1996) 565-574.
6. J.H. Zhang, T.C. Lee, W.S. Lau, J. Mater. Process. Technol. 63 (1997) 908-912.
7. C.S. Trueman, J. Huddleston, J. Eu. Ceram. Soc. 20 (2000) 1629-1635.
8. H. Hocheng, W.T. Lei, H.S. Hsu, J. Mater. Process. Technol. 63 (1997) 813-818.
9. A. Pitman, J. Huddleston, Br. Ceram. Trans. 99 [2] (2000)77-84.
10. C.C. Liu, J.L. Huang, Ceram. Int. 29 (2003) 679-687.
11. I. Puertas, C.J. Luis, Mater. Manuf. Process. 19 [6] (2004) 1041-1070.
12. C.J. Luis, I. Puertas, J. Mater. Process. Technol. 189 (2007) 301-309.
13. N. Mohri, Y. Fukuzawa, T. Tani, T. Sata, Ann. CIRP 51 [1] (2002) 161-164.
14. Y. Fukuzawa, T.Tani, N. Mohri, A. Muttamara, Int. J. Electr. Mach. 8 (2003) 57-61.
15. T.Tani, Y. Fuzawa, N. Mohri, N. Saito, M. Okada, J.Mater. Process. Technol. 149 (2004) 124-128.
16. Y.C. Lin, C.H.Cheng, B.L.Su, L.R. Hwang, Mater. Manuf. Process. 21 (2006) 922-929.
17. B.H. Yan, C.C.Wang, H.M. Chow, Y.C. Lin, Int. J. Mach. Tools Manuf. 40 (2000) 1403-1421.
18. J.S. Soni, G.Chakraverti, J. Mater. Process. Technol. 56 (1996) 439-451.
19. W. Natsu, M. Kunieda, N. Nishiwaki, Int. J. Electr. Mach. 9 (2004) 43-50.
20. Y.C. Lin, B.H. Yan, F.Y. Huang, J. Mater. Process. Technol. 115 (2001) 359-366.